Relations between codas in reflection and transmission data and their applications in seismic imaging

Kees Wapenaar, Deyan Draganov and Jan Thorbecke

Section of Applied Geophysics and Petrophysics, Centre for Technical Geoscience, Delft University of Technology (Corresponding author: C.P.A.Wapenaar@CTG.TUDelft.NL).

ABSTRACT

Codas in seismic data, due to internal multiple scattering, contain relevant information about the heterogeneities in the subsurface. Employing the information in the coda in seismic imaging may significantly improve the resolution. Codas occur in seismic reflection data as well as in transmission data. Whereas in seismic reflection data the sources are man-made, the sources in transmission data are usually natural sources, e.g. as in permanent monitoring of microseismic and/or earthquake events.

In this paper we derive two relations between reflection and transmission responses in 3-D inhomogeneous media. Based on these relations, we will show that the coda of the transmission response can be derived from the reflection response and, vice versa, that the reflection response, includings its coda, can be derived from the transmission response. The former relationship was derived by Herman (1992) and Wapenaar and Herrmann (1993) and the latter for horizontally layered media by Claerbout (1968). In the current paper we employ a unified approach for deriving both relationships, using reciprocity. Both results are valid for 3-D inhomogeneous media.

The reflection-to-transmission transform enables us to derive approximate inverse operators for seismic imaging in complex media in which internal multiple scattering plays a role. The transmission coda, required for these inverse operators, follows from the measured reflection data by employing a 3-D reflection-to-transmission transform. Hence, the imaging process for seismic reflection data in complex media is guided by the reflection data itself.

The transmission-to-reflection transform finds its application in acoustic daylight imaging. Responses from natural noise sources in the subsurface, observed by receivers at the surface, are transformed to reflection data, including the coda, that can be used for imaging the subsurface region between the surface and the noise sources in the subsurface. Our 3-D theory gives insight with respect to the required properties of the distribution of uncorrelated noise sources.

KEY WORDS: coda, internal multiples, reciprocity, one-way wave equation

INTRODUCTION

In this paper we present a unified approach for deriving two relationships between seismic reflection and transmission responses in 3-D inhomogeneous media. In both relations, the codas due to internal multiple scattering are included. We consider situations without and with a free surface on top of the configuration; below a specific depth level we assume that the medium is homogeneous.

The relations between reflection and transmission responses are the basis for deriving the *coda* of the transmission response from the reflection response and, vice versa, the reflection response from the transmission response. The former relation is useful for deriving seismic imaging schemes that take internal multiple scattering into account. The latter relation is relevant for 'acoustic daylight imaging', i.e., imaging the subsurface from passive recordings of the transmission responses of natural noise sources in the subsurface (Rickett and Claerbout, 1999).

ONE-WAY RECIPROCITY THEOREM

We use acoustic reciprocity as a starting point to derive the relations between the reflection and transmission responses. Acoustic reciprocity formulates a relation between two acoustic states in one and the same domain [(de Hoop, 1988), (Fokkema and van den Berg, 1993)]. The two states will be distinguished by subscripts A and B. Usually reciprocity theorems apply to the full wave fields in both states. As an alternative, Wapenaar and Grimbergen (1996) derived reciprocity theorems for one-way (i.e. downgoing and upgoing) wave fields. For a plan-parallel domain $\mathcal{D}$ embedded between surfaces $\partial\mathcal{D}_0$ and $\partial\mathcal{D}_m$ at depth levels $x_{3,0}+\epsilon$ and $x_{3,m}-\epsilon$, respectively (with $x_{3,m} > x_{3,0}$ and ϵ a vanishing positive constant), the one-way reciprocity theorem of the correlation type reads in the space-frequency $(\mathbf{x}, \omega)$ domain

$$\int_{\partial\mathcal{D}_0} \{(P_A^+)^* P_B^+ - (P_A^-)^* P_B^-\} \mathrm{d}^2\mathbf{x} = \int_{\partial\mathcal{D}_m} \{(P_A^+)^* P_B^+ - (P_A^-)^* P_B^-\} \mathrm{d}^2\mathbf{x}, \qquad (1)$$

where P^+ and P^- are flux-normalized downgoing and upgoing wave fields, respectively, and * denotes complex conjugation. In equation (1) it has been

assumed that the medium parameters in both states are identical, lossless and 3-D inhomogeneous and that the domain $\mathcal{D}$ is source-free. Furthermore, evanescent wave modes are neglected.

THE REFLECTION-TO-TRANSMISSION TRANSFORM

Relation between reflection and transmission responses without free surface multiples

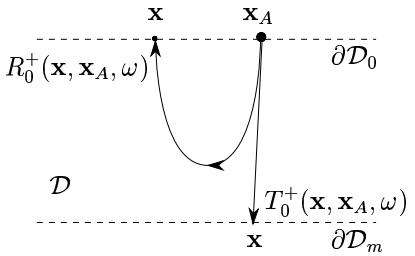

Fig. 1: *Domain $\mathcal{D}$ between surfaces $\partial\mathcal{D}_0$ and $\partial\mathcal{D}_m$. The medium in $\mathcal{D}$ is inhomogeneous in the x_1-, x_2- and x_3-directions. The half-spaces above $\partial\mathcal{D}_0$ and below $\partial\mathcal{D}_m$ are homogeneous.*

We employ equation (1) to derive the first relation between the reflection and transmission responses of the medium in domain $\mathcal{D}$. To this end we consider the configuration of Figure 1, in which *both* half-spaces above $\partial\mathcal{D}_0$ and below $\partial\mathcal{D}_m$ are homogeneous. For states A and B we choose sources for downgoing waves at $\mathbf{x}_A$ and $\mathbf{x}_B$ in the upper half-space, just above $\partial\mathcal{D}_0$, that is, we define $\mathbf{x}_A = (\mathbf{x}_{H,A}, x_{3,0})$ and $\mathbf{x}_B = (\mathbf{x}_{H,B}, x_{3,0})$. Here we used the subscript $_H$ to denote the horizontal coordinates, i.e., $\mathbf{x}_H = (x_1, x_2)$. Hence, $\mathbf{x}_{H,A}$ denotes the horizontal coordinates of $\mathbf{x}_A$, i.e., $\mathbf{x}_{H,A} = (x_{1,A}, x_{2,A})$, etc. Hence, for $\mathbf{x}$ at $\partial\mathcal{D}_0$ we have

$$P_A^+(\mathbf{x},\mathbf{x}_A,\omega) = \delta(\mathbf{x}_H - \mathbf{x}_{H,A})s_A(\omega), \quad (2)$$

$$P_B^+(\mathbf{x},\mathbf{x}_B,\omega) = \delta(\mathbf{x}_H - \mathbf{x}_{H,B})s_B(\omega), \quad (3)$$

$$P_A^-(\mathbf{x},\mathbf{x}_A,\omega) = R_0^+(\mathbf{x},\mathbf{x}_A,\omega)s_A(\omega), \quad (4)$$

$$P_B^-(\mathbf{x},\mathbf{x}_B,\omega) = R_0^+(\mathbf{x},\mathbf{x}_B,\omega)s_B(\omega), \quad (5)$$

where $s_A(\omega)$ and $s_B(\omega)$ are the source spectra for both states. $R_0^+(\mathbf{x},\mathbf{x}_A,\omega)$ is the reflection response of the inhomogeneous medium in $\mathcal{D}$, including all internal multiples, for a source at $\mathbf{x}_A$ and a receiver at $\mathbf{x}$ (Figure 1). A similar remark applies to $R_0^+(\mathbf{x},\mathbf{x}_B,\omega)$. The subscript $_0$ denotes that no free surface multiples are included. For $\mathbf{x}$ at $\partial\mathcal{D}_m$ we have

$$P_A^+(\mathbf{x},\mathbf{x}_A,\omega) = T_0^+(\mathbf{x},\mathbf{x}_A,\omega)s_A(\omega), \quad (6)$$

$$P_B^+(\mathbf{x},\mathbf{x}_B,\omega) = T_0^+(\mathbf{x},\mathbf{x}_B,\omega)s_B(\omega), \quad (7)$$

$$P_A^-(\mathbf{x},\mathbf{x}_A,\omega) = P_B^-(\mathbf{x},\mathbf{x}_B,\omega) = 0, \quad (8)$$

where $T_0^+(\mathbf{x},\mathbf{x}_A,\omega)$ is the transmission response of the inhomogeneous medium in $\mathcal{D}$, including all internal multiples (Figure 1). Substitution into equation (1) and dividing both sides of the equation by $s_A^*(\omega)s_B(\omega)$ yields

$$\int_{\partial\mathcal{D}_m} \{T_0^+(\mathbf{x},\mathbf{x}_A,\omega)\}^* T_0^+(\mathbf{x},\mathbf{x}_B,\omega)\mathrm{d}^2\mathbf{x} = \quad (9)$$
$$\delta(\mathbf{x}_{H,B} - \mathbf{x}_{H,A}) - \int_{\partial\mathcal{D}_0} \{R_0^+(\mathbf{x},\mathbf{x}_A,\omega)\}^* R_0^+(\mathbf{x},\mathbf{x}_B,\omega)\mathrm{d}^2\mathbf{x}.$$

When the reflection response $R_0^+(\mathbf{x},\mathbf{x}_A,\omega)$ without free surface multiples is known [for example after applying surface multiple elimination to the measured reflection response (Verschuur et al., 1992)], equation (9) may be seen as an implicit equation for the transmission response $T_0^+(\mathbf{x},\mathbf{x}_A,\omega)$. Similar expressions have been derived before by Herman (1992) using a two-way reciprocity theorem and by Wapenaar and Herrmann (1993) using the one-way reciprocity theorem (equation 1). There is no unique way to resolve the transmission response $T_0^+(\mathbf{x},\mathbf{x}_A,\omega)$ from the left-hand side of equation (9). In the following subsection we indicate how the transmission *coda* can be resolved from this equation.

Resolving the transmission coda from the reflection response

We rewrite equation (9) in matrix form, according to

$$\{\mathbf{T}_0^+(x_{3,m},x_{3,0},\omega)\}^\dagger \mathbf{T}_0^+(x_{3,m},x_{3,0},\omega) = \quad (10)$$
$$\mathbf{I} - \{\mathbf{R}_0^+(x_{3,0},\omega)\}^\dagger \mathbf{R}_0^+(x_{3,0},\omega).$$

A column of matrix $\mathbf{R}_0^+(x_{3,0},\omega)$ contains the discretized version of $R_0^+(\mathbf{x},\mathbf{x}_A,\omega)$ for a fixed source position $\mathbf{x}_A$ and a range of receiver positions $\mathbf{x}$ at $x_{3,0}$, etc. (Berkhout, 1982). $\mathbf{I}$ is an identity matrix of the same size as $\mathbf{R}_0^+(x_{3,0},\omega)$ and $\mathbf{T}_0^+(x_{3,m},x_{3,0},\omega)$. Finally, the dagger † denotes transposition and complex conjugation. For the transmission response we write

$$\mathbf{T}_0^+(x_{3,m},x_{3,0},\omega) = \mathbf{W}_p^+(x_{3,m},x_{3,0},\omega)\mathbf{C}(\omega), \quad (11)$$

where $\mathbf{W}_p^+(x_{3,m},x_{3,0},\omega)$ is the primary propagator for downgoing waves between depth levels $x_{3,0}$ and $x_{3,m}$ and where $\mathbf{C}(\omega)$ accounts for the coda due to multiple scattering caused by the inhomogeneities between these two depth levels. The primary propagator is unitary, according to

$$\{\mathbf{W}_p^+(x_{3,m},x_{3,0},\omega)\}^\dagger \mathbf{W}_p^+(x_{3,m},x_{3,0},\omega) = \mathbf{I}. \quad (12)$$

Hence, upon substitution of equation (11) into equation (10), using equation (12), we obtain

$$\mathbf{C}^\dagger(\omega)\mathbf{C}(\omega) = \mathbf{I} - \{\mathbf{R}_0^+(x_{3,0},\omega)\}^\dagger \mathbf{R}_0^+(x_{3,0},\omega). \quad (13)$$

This equation states that the auto-correlation of transmission coda matrix, i.e. $\mathbf{C}^\dagger(\omega)\mathbf{C}(\omega)$, can be obtained from the auto-correlation of the reflection matrix. Next we need to resolve $\mathbf{C}(\omega)$ from $\mathbf{C}^\dagger(\omega)\mathbf{C}(\omega)$. To this end we assume that $\mathbf{C}(\omega)$ can be written as

$$\mathbf{C}(\omega) = \mathbf{L}(\omega)\Lambda(\omega)\mathbf{L}^\dagger(\omega), \quad (14)$$

where

$$\Lambda(\omega) = \begin{pmatrix} \mathrm{e}^{-A_1(\omega)} & 0 & \dots & 0 \\ 0 & \mathrm{e}^{-A_2(\omega)} & \dots & 0 \\ \dots & \dots & \dots & \dots \\ 0 & 0 & \dots & \mathrm{e}^{-A_N(\omega)} \end{pmatrix}, \quad (15)$$

with $A_1(\omega)$, $A_2(\omega)$, ..., $A_N(\omega)$ being the temporal Fourier transforms of causal functions. For horizontally layered media it is indeed possible to write the matrix $\mathbf{C}(\omega)$ in this way; for 3-D inhomogeneous media this remains to be investigated. With this assumption, $\mathbf{C}^\dagger(\omega)\mathbf{C}(\omega)$ can be written as

$$\mathbf{C}^\dagger(\omega)\mathbf{C}(\omega) = \mathbf{L}(\omega)\Lambda^\dagger(\omega)\Lambda(\omega)\mathbf{L}^\dagger(\omega), \quad (16)$$

where

$$\Lambda^\dagger(\omega)\Lambda(\omega) = \quad (17)$$

$$\begin{pmatrix} \mathrm{e}^{-2\Re\{A_1(\omega)\}} & 0 & \dots & 0 \\ 0 & \mathrm{e}^{-2\Re\{A_2(\omega)\}} & \dots & 0 \\ \dots & \dots & \dots & \dots \\ 0 & 0 & \dots & \mathrm{e}^{-2\Re\{A_N(\omega)\}} \end{pmatrix},$$

with $\Re\{\cdot\}$ denoting the real part. Since the functions $A_n(\omega)$ correspond to causal functions in the time domain, they can be reconstructed from their real part via the Hilbert transform, according to

$$A_n(\omega) = \Re\{A_n(\omega)\} + \frac{1}{j\pi}\int_{-\infty}^{\infty} \frac{\Re\{A_{n'}(\omega')\}}{\omega - \omega'}\,\mathrm{d}\omega', \quad (18)$$

where $\Re\{A_{n'}(\omega')\}$ is taken from matrices like the one in equation (17) but at different frequencies. In general, the eigenvalue number n' will change with changing frequency ω'.

Hence, resolving the transmission coda $\mathbf{C}(\omega)$ from the reflection response matrix $\mathbf{R}_0^+(x_{3,0},\omega)$ comes to the following steps:

- compute $\{\mathbf{R}_0^+(x_{3,0},\omega)\}^\dagger\mathbf{R}_0^+(x_{3,0},\omega)$, which yields $\mathbf{C}^\dagger(\omega)\mathbf{C}(\omega)$ according to equation (13),
- apply eigenvalue decomposition to $\mathbf{C}^\dagger(\omega)\mathbf{C}(\omega)$, yielding $\Lambda^\dagger(\omega)\Lambda(\omega)$ according to equation (16),
- take the logarithm of the diagonal elements of $\Lambda^\dagger(\omega)\Lambda(\omega)$, yielding $-2\Re\{A_n(\omega)\}$ according to equation (17),
- reconstruct $A_n(\omega)$ from $\Re\{A_n(\omega)\}$ according to equation (18),
- insert $A_n(\omega)$ into $\Lambda(\omega)$ (equation (15)) and reconstruct $\mathbf{C}(\omega)$ from $\Lambda(\omega)$, using equation (14).

Assuming the primary propagator $\mathbf{W}_p^+(x_{3,m},x_{3,0},\omega)$ is known (for example from traveltime tomography), the transmission matrix $\mathbf{T}_0^+(x_{3,m},x_{3,0},\omega)$ is finally obtained from equation (11). We are currently investigating this approach for the 2-D and 3-D situation. Here we illustrate it with a 1-D example.

Layer	Velocity (m/s)	Density (kg/m^3)	Thickness (m)
1	1000	1000	100
2	4000	1000	100
3	2000	1000	100
4	1000	1000	100
5	2000	1000	100
6	4000	1000	100
7	2000	1000	100

TABLE 1: Seven-layer medium

For the seven-layer medium of Table 1, Figure 2 shows the plane wave transmission response, i.e. the inverse Fourier transform of $T_0^+(x_{3,m},x_{3,0},\omega)$. For the same medium, the plane wave reflection response $R_0^+(x_{3,0},\omega)$, is shown in the time domain in Figure 3. We will now show step by step how the transmission response can be obtained from the reflection response and the primary propagator $W_p^+(x_{3,m},x_{3,0},\omega)$. First we obtain $C^*(\omega)C(\omega)$ from the 1-D version of equation (13), according to

$$C^*(\omega)C(\omega) = 1 - \{R_0^+(x_{3,0},\omega)\}^* R_0^+(x_{3,0},\omega). \quad (19)$$

The time domain version of the right-hand side is shown in Figure 4. Since $C^*(\omega)C(\omega)$ is a scalar function we can replace the eigenvalue decomposition [equations (16) and (17)] by $C^*(\omega)C(\omega) = \mathrm{e}^{-2\Re\{A(\omega)\}}$, hence we obtain $2\Re\{A(\omega)\}$ from

$$2\Re\{A(\omega)\} = -\ln\Big(C^*(\omega)C(\omega)\Big). \quad (20)$$

We rename the left-hand side $2A_R(\omega)$, denoting the real part of $A(\omega)$; its time domain version is shown in Figure 5. According to equation (18), $A(\omega)$ can be reconstructed from its real part. This is equivalent to taking the causal part of $2A_R(t)$ in the time domain, see Figure 6, where $H(t)$ is the Heaviside function. Now that $A(\omega)$ has been found, the coda is obtained from

$$C(\omega) = \mathrm{e}^{-A(\omega)}, \quad (21)$$

which is the 1-D equivalent of equations (14) and (15). Its time domain version is shown in Figure 7. According to the 1-D equivalent of equation (11),

$$\begin{aligned} T_0^+(x_{3,m},x_{3,0},\omega) &= W_p^+(x_{3,m},x_{3,0},\omega)C(\omega) \\ &= \mathrm{e}^{-j\omega t_0}C(\omega) \end{aligned} \quad (22)$$

(t_0 denotes the primary traveltime), the transmission response can now be reconstructed. In the time domain this is accomplished by a time-shift of the coda over t_0, see Figure 8. Figure 9 shows the difference between the true transmission response of Figure 2 and the reconstructed version of Figure 8. Note the perfect reconstruction (the vertical scale is in the range of 10^{-5}).

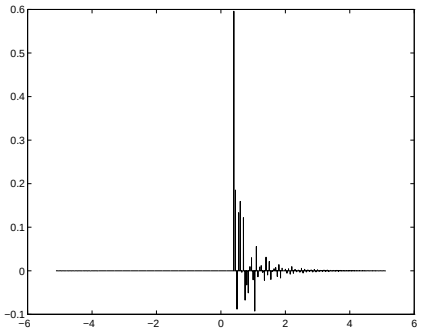

Fig. 2: Transmission response $T_0^+(x_{3,m}, x_{3,0}, t)$ for the seven-layer medium in Table 1.

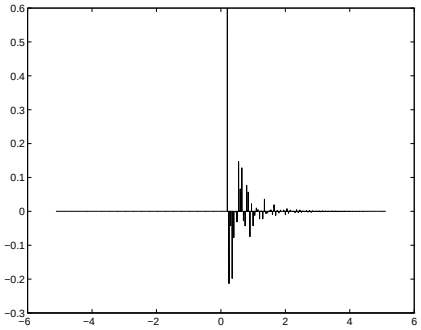

Fig. 3: Reflection response $R_0^+(x_{3,0}, t)$.

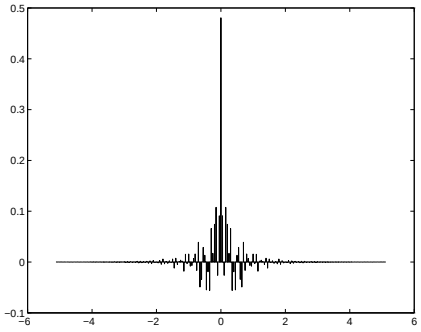

Fig. 4: $\delta(t) - R_0^+(x_{3,0}, -t) * R_0^+(x_{3,0}, t)$.

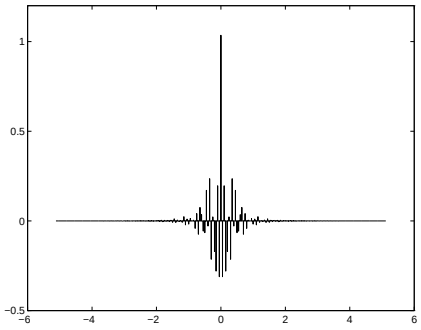

Fig. 5: The function $2A_R(t)$.

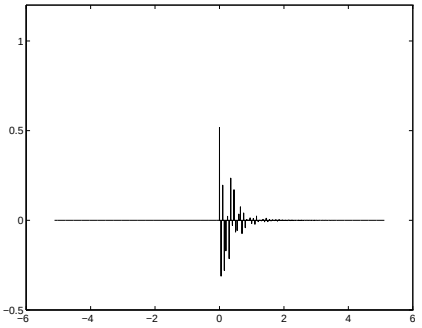

Fig. 6: $A(t) = H(t)2A_R(t)$.

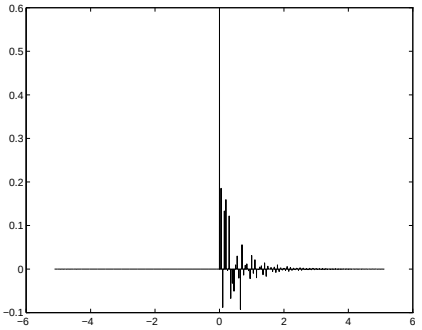

Fig. 7: The coda $C(t)$.

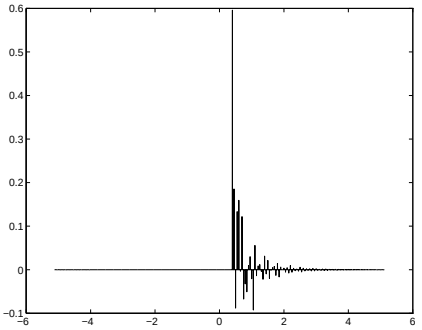

Fig. 8: The reconstructed transmission response: $T_0^+(x_{3,m}, x_{3,0}, t) = C(t - t_0)$.

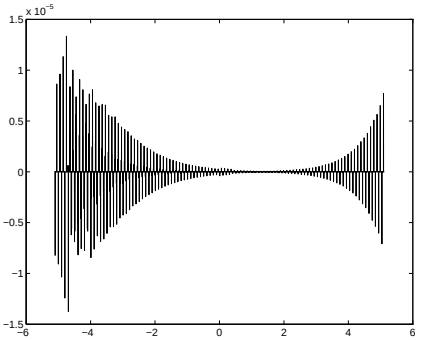

Fig. 9: Difference between the true transmission response of Figure 2 and its reconstructed version of Figure 8 (note that the vertical scale is in the range of 10^{-5}).

The inverse transmission coda

Using the matrix notation of equation (10), we introduce the inverse transmission response $\mathbf{T}_0^{+,\mathrm{inv}}(x_{3,0}, x_{3,m}, \omega)$, according to

$$\mathbf{T}_0^{+,\mathrm{inv}}(x_{3,0}, x_{3,m}, \omega)\mathbf{T}_0^{+}(x_{3,m}, x_{3,0}, \omega) = \mathbf{I}. \quad (23)$$

By rewriting equation (10) as follows

$$\Big[\mathbf{I} - \{\mathbf{R}_0^{+}(x_{3,0}, \omega)\}^{\dagger}\mathbf{R}_0^{+}(x_{3,0}, \omega)\Big]^{-1} \times \quad (24)$$
$$\{\mathbf{T}_0^{+}(x_{3,m}, x_{3,0}, \omega)\}^{\dagger}\mathbf{T}_0^{+}(x_{3,m}, x_{3,0}, \omega) = \mathbf{I}$$

and comparing this with equation (23), we find that the inverse transmission response is given by

$$\mathbf{T}_0^{+,\mathrm{inv}}(x_{3,0}, x_{3,m}, \omega) = \quad (25)$$
$$\Big[\mathbf{I} - \{\mathbf{R}_0^{+}(x_{3,0}, \omega)\}^{\dagger}\mathbf{R}_0^{+}(x_{3,0}, \omega)\Big]^{-1}\{\mathbf{T}_0^{+}(x_{3,m}, x_{3,0}, \omega)\}^{\dagger}$$

(Wapenaar and Herrmann, 1993). Using a Neumann expansion, this becomes

$$\langle \mathbf{T}_0^{+,\mathrm{inv}}(x_{3,0}, x_{3,m}, \omega)\rangle = \quad (26)$$
$$\sum_{i=0}^{i_{\max}} \Big[\{\mathbf{R}_0^{+}(x_{3,0}, \omega)\}^{\dagger}\mathbf{R}_0^{+}(x_{3,0}, \omega)\Big]^{i}\{\mathbf{T}_0^{+}(x_{3,m}, x_{3,0}, \omega)\}^{\dagger}$$

where $\langle\cdot\rangle$ denotes an estimate. For $i_{\max} = 0$, equation (26) reduces to $\langle \mathbf{T}_0^{+,\mathrm{inv}}(x_{3,0}, x_{3,m}, \omega)\rangle = \{\mathbf{T}_0^{+}(x_{3,m}, x_{3,0}, \omega)\}^{\dagger}$, which is the usual matched filter approximation. In a similar way we can derive from equation (13) for the inverse coda

$$\langle \mathbf{C}^{\mathrm{inv}}(\omega)\rangle = \quad (27)$$
$$\sum_{i=0}^{i_{\max}} \Big[\{\mathbf{R}_0^{+}(x_{3,0}, \omega)\}^{\dagger}\mathbf{R}_0^{+}(x_{3,0}, \omega)\Big]^{i}\mathbf{C}^{\dagger}(\omega).$$

For $i_{\max} = 0$ this reduces to $\langle \mathbf{C}^{\mathrm{inv}}(\omega)\rangle = \mathbf{C}^{\dagger}(\omega)$. Note that in equation (27) $\langle \mathbf{C}^{\mathrm{inv}}(\omega)\rangle$ is derived from the reflection data only, whereas in equation (26) $\langle \mathbf{T}_0^{+,\mathrm{inv}}(x_{3,0}, x_{3,m}, \omega)\rangle$ is derived from the reflection data as well as from the primary propagator $\mathbf{W}_p^{+}(x_{3,m}, x_{3,0}, \omega)$ (which is contained in $\mathbf{T}_0^{+}(x_{3,m}, x_{3,0}, \omega)$, according to equation (11)). We illustrate the inversion of the coda with a 1-D example. The 1-D version of equation (27) reads

$$\langle C^{\mathrm{inv}}(\omega)\rangle = \quad (28)$$
$$\sum_{i=0}^{i_{\max}} \Big[\{R_0^{+}(x_{3,0}, \omega)\}^{*}R_0^{+}(x_{3,0}, \omega)\Big]^{i}C^{*}(\omega).$$

For $i_{\max} = 0$ this reduces in the time domain to a time-reversal of $C(t)$ of Figure 7. The result is shown in Figure 10. For $i_{\max} = 5, 20, 100$ the results are shown in the time domain in Figures 11, 12 and 13, respectively. Note that $\langle C^{\mathrm{inv}}(\omega)\rangle$ changes from an anti-causal function for $i_{\max} = 0$ to a causal function for $i_{\max} \to \infty$.

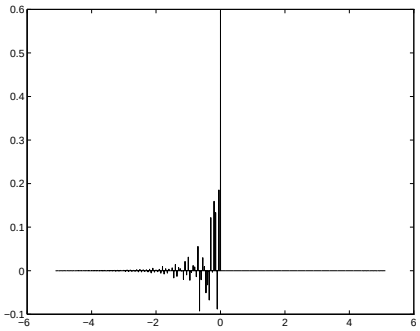

Fig. 10: Approximate inverse coda for $i_{\max} = 0$: $\langle C^{\mathrm{inv}}(t)\rangle = C(-t)$.

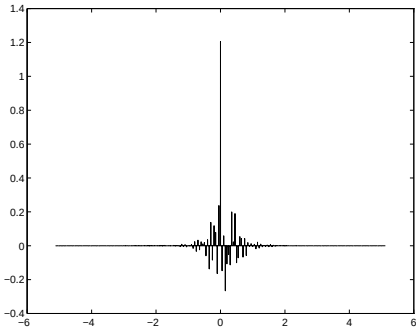

Fig. 11: Approximate inverse coda for $i_{\max} = 5$.

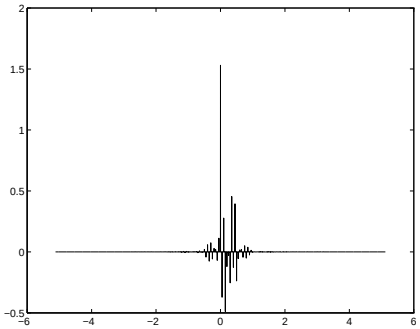

Fig. 12: Approximate inverse coda for $i_{\max} = 20$.

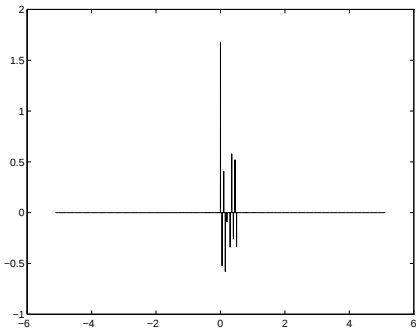

Fig. 13: Approximate inverse coda for $i_{\max} = 100$.

Application in seismic imaging

The response of a reflector at depth level $x_{3,m}$, observed at depth level $x_{3,0}$, reads

$$\mathbf{P}_m^-(x_{3,0},\omega) = \mathbf{T}_0^-(x_{3,0},x_{3,m},\omega)\mathbf{r}(x_{3,m})\mathbf{T}_0^+(x_{3,m},x_{3,0},\omega), \quad (29)$$

with $\mathbf{T}_0^-(x_{3,0},x_{3,m},\omega) = \{\mathbf{T}_0^+(x_{3,m},x_{3,0},\omega)\}^t$ and $\mathbf{r}(x_{3,m})$ being a local reflection matrix (i.e., only related to depth level $x_{3,m}$). Note that $\mathbf{P}_m^-(x_{3,0},\omega)$, as defined in equation (29), contains the effects of internal multiple scattering due to inhomogeneities between the depth levels $x_{3,0}$ and $x_{3,m}$. By applying the inverse transmission responses to $\mathbf{P}_m^-(x_{3,0},\omega)$ we obtain the reflection matrix $\mathbf{r}(x_{3,m})$, according to

$$\mathbf{T}_0^{-,\mathrm{inv}}(x_{3,m},x_{3,0},\omega)\mathbf{P}_m^-(x_{3,0},\omega)\mathbf{T}_0^{+,\mathrm{inv}}(x_{3,0},x_{3,m},\omega), \quad (30)$$

with $\mathbf{T}_0^{-,\mathrm{inv}}(x_{3,m},x_{3,0},\omega) = \{\mathbf{T}_0^{+,\mathrm{inv}}(x_{3,0},x_{3,m},\omega)\}^t$. Alternatively, when we apply the inverse codas to $\mathbf{P}_m^-(x_{3,0},\omega)$ we obtain

$$\mathbf{W}_p^-(x_{3,0},x_{3,m},\omega)\mathbf{r}(x_{3,m})\mathbf{W}_p^+(x_{3,m},x_{3,0},\omega) = \{\mathbf{C}^{\mathrm{inv}}(\omega)\}^t\mathbf{P}_m^-(x_{3,0},\omega)\mathbf{C}^{\mathrm{inv}}(\omega), \quad (31)$$

which follows by substituting equation (11) into (29) and using the above mentioned symmetry relations. The left-hand side of equation (31) represents the primary response of the reflector at depth level $x_{3,m}$, observed at depth level $x_{3,0}$. Hence, the inverse coda matrices in equation (31) remove the internal multiples from the response $\mathbf{P}_m^-(x_{3,0},\omega)$, defined in equation (29). We illustrate this with a 1-D example. The 1-D equivalent of equation (29) is given by

$$P_m^-(x_{3,0},\omega) = T_0^-(x_{3,0},x_{3,m},\omega)r(x_{3,m})T_0^+(x_{3,m},x_{3,0},\omega), \quad (32)$$

The response of a reflector at $x_{3,m} = 700$m (the lower boundary of the layered medium of Table 1), with $r(x_{3,m}) = 1$, is shown in the time domain in Figure 14. This is the auto-convolution of the transmission response of Figure 2. The 1-D version of equation (31) reads

$$W_p^-(x_{3,0},x_{3,m},\omega)r(x_{3,m})W_p^+(x_{3,m},x_{3,0},\omega) = \mathrm{e}^{-2j\omega t_0}r(x_{3,m}) = C^{\mathrm{inv}}(\omega)P_m^-(x_{3,0},\omega)C^{\mathrm{inv}}(\omega). \quad (33)$$

The result for $i_{\max} = 0$, for which $\langle C^{\mathrm{inv}}(\omega)\rangle = C^*(\omega)$, is shown in the time domain in Figure 15. Note that the approximate inverse codas have a zero-phasing effect, but they do not suppress the internal multiples. In Figure 16 the result is shown of applying $\langle C^{\mathrm{inv}}(\omega)\rangle$ for $i_{\max} = 100$: the internal multiples are perfectly removed and the strength of the reflector ($r(x_{3,m}) = 1$) has been correctly recovered. It should be noted that we have considered an idealized situation in the sense that we estimated $\langle C^{\mathrm{inv}}(\omega)\rangle$ from the reflection response of the medium between $x_{3,0}$ and $x_{3,m}$ (Figure 3), without the response of the reflector at $x_{3,m} = 700$m (Figure 14) or any reflectors below $x_{3,m} = 700$m. In practice $\langle C^{\mathrm{inv}}(\omega)\rangle$ should be estimated from a carefully windowed version of the reflection response.

The 1-D examples have shown that the reflection-to-transmission transform has the potential to suppress the effects of internal multiple scattering in seismic imaging, using an inverse coda derived from the reflection reponse itself. For correct depth positioning the inverse primary propagator should be estimated from traveltime information (as usual). We are currently developing the 3-D extension of this approach. For comparison, in the imaging scheme proposed by Weglein et al. (2000), the full inverse operator (primaries as well as internal multiples) is estimated directly from the reflection measurements. The advantages and disadvantages of both methods with respect to accuracy, stability, etc. remain to be investigated.

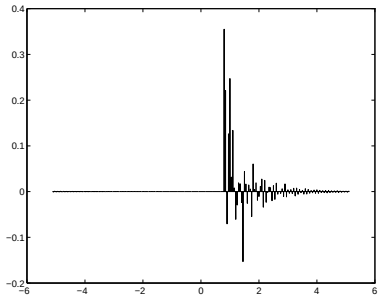

Fig. 14: Reflection response $P_m^-(x_{3,0},t) = T_0^-(x_{3,0},x_{3,m},t) * T_0^+(x_{3,m},x_{3,0},t)$.

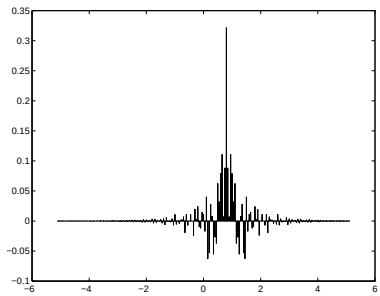

Fig. 15: $C(-t) * P_m^-(x_{3,0},t) * C(-t)$.

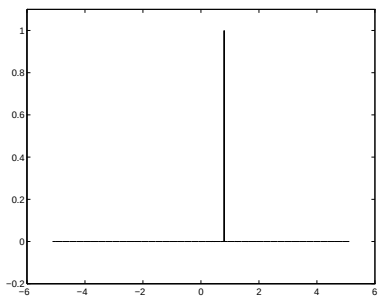

Fig. 16: $\langle C^{\mathrm{inv}}(t)\rangle * P_m^-(x_{3,0},t) * \langle C^{\mathrm{inv}}(t)\rangle$. Note that the internal multiples have been removed.

THE TRANSMISSION-TO-REFLECTION TRANSFORM

Relation between reflection and transmission responses with free surface multiples

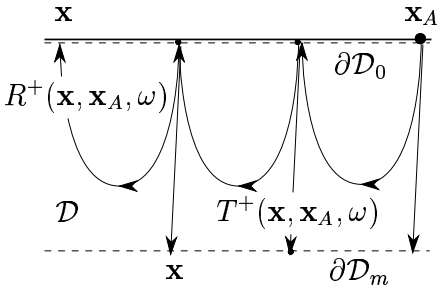

Fig. 17: *Domain $\mathcal{D}$ between surfaces $\partial\mathcal{D}_0$ and $\partial\mathcal{D}_m$. The medium in $\mathcal{D}$ is inhomogeneous in the x_1-, x_2- and x_3-directions. There is a free surface just above $\partial\mathcal{D}_0$; the half-space below $\partial\mathcal{D}_m$ is again homogeneous.*

We employ again equation (1) to derive the second relation between the reflection and transmission responses of the medium in domain $\mathcal{D}$. This time we consider the configuration of Figure 17, in which we choose a free surface at $x_{3,0}$, i.e., just above $\partial\mathcal{D}_0$, and a homogeneous half-space below $\partial\mathcal{D}_m$. The source points $\mathbf{x}_A$ and $\mathbf{x}_B$ are chosen as before. Hence, for $\mathbf{x}$ at $\partial\mathcal{D}_0$ we now have

$$P_A^+(\mathbf{x},\mathbf{x}_A,\omega) = \delta(\mathbf{x}_H-\mathbf{x}_{H,A})s_A(\omega) + rP_A^-(\mathbf{x},\mathbf{x}_A,\omega), \quad (34)$$

$$P_B^+(\mathbf{x},\mathbf{x}_B,\omega) = \delta(\mathbf{x}_H-\mathbf{x}_{H,B})s_B(\omega) + rP_B^-(\mathbf{x},\mathbf{x}_B,\omega), \quad (35)$$

$$P_A^-(\mathbf{x},\mathbf{x}_A,\omega) = R^+(\mathbf{x},\mathbf{x}_A,\omega)s_A(\omega), \quad (36)$$

$$P_B^-(\mathbf{x},\mathbf{x}_B,\omega) = R^+(\mathbf{x},\mathbf{x}_B,\omega)s_B(\omega), \quad (37)$$

where r is the reflection coefficient of the free surface ($r=-1$) and $R^+(\mathbf{x},\mathbf{x}_A,\omega)$ is the reflection response of the inhomogeneous medium in $\mathcal{D}$, including all internal and free surface multiples (Figure 17). For $\mathbf{x}$ at $\partial\mathcal{D}_m$ we have

$$P_A^+(\mathbf{x},\mathbf{x}_A,\omega) = T^+(\mathbf{x},\mathbf{x}_A,\omega)s_A(\omega), \quad (38)$$

$$P_B^+(\mathbf{x},\mathbf{x}_B,\omega) = T^+(\mathbf{x},\mathbf{x}_B,\omega)s_B(\omega), \quad (39)$$

$$P_A^-(\mathbf{x},\mathbf{x}_A,\omega) = P_B^-(\mathbf{x},\mathbf{x}_B,\omega) = 0, \quad (40)$$

where $T^+(\mathbf{x},\mathbf{x}_A,\omega)$ is the transmission response of the inhomogeneous medium in $\mathcal{D}$, including all internal and free surface multiples (Figure 17). Substitution into equation (1), using $R^+(\mathbf{x}_A,\mathbf{x}_B,\omega) = R^+(\mathbf{x}_B,\mathbf{x}_A,\omega)$ and $T^-(\mathbf{x}_A,\mathbf{x},\omega) = T^+(\mathbf{x},\mathbf{x}_A,\omega)$, and dividing both sides of the equation by $s_A^*(\omega)s_B(\omega)$ yields

$$2\Re\big[R^+(\mathbf{x}_A,\mathbf{x}_B,\omega)\big] = \delta(\mathbf{x}_{H,B}-\mathbf{x}_{H,A}) - \int_{\partial\mathcal{D}_m}\{T^-(\mathbf{x}_A,\mathbf{x},\omega)\}^*T^-(\mathbf{x}_B,\mathbf{x},\omega)\mathrm{d}^2\mathbf{x}. \quad (41)$$

When the transmission responses $T^-(\mathbf{x}_A,\mathbf{x},\omega)$ and $T^-(\mathbf{x}_B,\mathbf{x},\omega)$ with free surface multiples are known for a sufficient range of $\mathbf{x}$-values (for example from passive measurements of natural noise sources in the subsurface, see the discussion below), equation (41) is an *explicit* expression for the real part of the reflection response $R^+(\mathbf{x}_A,\mathbf{x}_B,\omega)$. Since the reflection response in the time domain is causal, the imaginary part of $R^+(\mathbf{x}_A,\mathbf{x}_B,\omega)$ is obtained via the Hilbert transform of the real part. Alternatively, $2\Re\{R^+(\mathbf{x}_A,\mathbf{x}_B,\omega)\}$ can be transformed to the time domain and subsequently be multiplied by the Heaviside step-function (i.e., taking the causal part), yielding the time domain version of $R^+(\mathbf{x}_A,\mathbf{x}_B,\omega)$.

Equation (41) is illustrated with a 2-D numerical experiment. The transmission response $T^-(\mathbf{x}_A,\mathbf{x},\omega)$ of the double-syncline model in Figure 18 is shown in the time domain in Figure 19a for a fixed source at $\mathbf{x}=(0,800)$ and a range of receiver positions $\mathbf{x}_A$ at the acquisition surface. Figure 19b shows the result (again in the time domain) of the integral in the right-hand side of equation (41) (times -1), for $\mathbf{x}_B=(0,0)$ and all $\mathbf{x}_A$ at the acquisition surface. The cross in the centre is a band-limited representation of a delta function (bear in mind that evanescent waves are neglected), which is compensated by the delta function in the right-hand side of equation (41). Figure 19c shows the causal part of the data in Figure 19b, after muting the bandlimited delta function. This is the reflection response $R^+(\mathbf{x}_A,\mathbf{x}_B,\omega)$ for a source at $\mathbf{x}_B=(0,0)$ and receivers at all $\mathbf{x}_A$ at the acquisition surface. This result matches quite accurately the directly modeled reflection response of the syncline model (not shown). Note that the coda due to internal multiple scattering between the two synclines in Figure 18 is clearly visible in Figure 19c. The 1-D version of quation (41), i.e., $2\Re\big[R^+(\omega)\big] = 1-\{T^-(\omega)\}^*T^-(\omega)$, was previously derived (in the z-transform domain) by Claerbout (1968). Assuming the 1-D assumption is justified this equation implies that, when a natural noise source in the Earth's subsurface emits plane waves to the surface, passive measurements of the noise at the surface suffice to compute the reflection response of the Earth's subsurface ('acoustic daylight imaging'). Claerbout conjectured for the

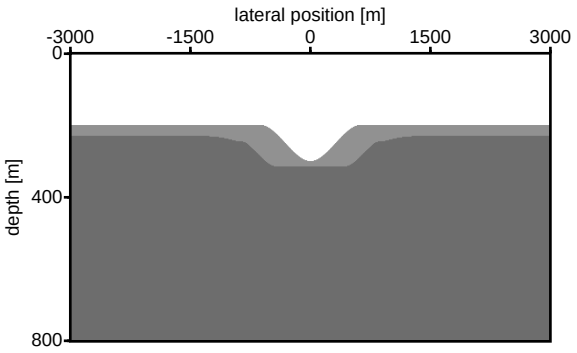

Fig. 18: *Double syncline model*

3-D situation that 'by cross-correlating noise traces recorded at two locations on the surface, we can construct the wave field that would be recorded at one of the locations if there was a source at the other'. Note that with equation (41) we nearly achieved a proof of Claerbout's conjecture. The term $\{T^-(\mathbf{x}_A,\mathbf{x},\omega)\}^*T^-(\mathbf{x}_B,\mathbf{x},\omega)$ represents the cross-correlation of traces recorded at two locations ($\mathbf{x}_A$ and $\mathbf{x}_B$) on the surface for a source at $\mathbf{x}$ in the subsurface; the term $R^+(\mathbf{x}_A,\mathbf{x}_B,\omega)$ is the wave field that would be recorded at one of the locations ($\mathbf{x}_A$) if there was a source at the other ($\mathbf{x}_B$). The main discrepancy with the conjecture is the integral in equation (41) over all possible source positions $\mathbf{x}$ at surface $\partial\mathcal{D}_m$. It can not be evaluated in practice because the transmission responses are not available for all individual source positions $\mathbf{x}$. However, if we assume uncorrelated noise sources at $\partial\mathcal{D}_m$, the integral of the product $\{T^-(\mathbf{x}_A,\mathbf{x},\omega)\}^*T^-(\mathbf{x}_B,\mathbf{x},\omega)$ can be rewritten as a product of integrals, each of these integrals describing the transmission response of the total distribution of noise sources. This completes the proof of Claerbout's conjecture.

CONCLUSIONS

We have used the reciprocity theorem of the correlation type for one-way wave fields to derive two relations between the transmission and reflection responses of an arbitrary 3-D inhomogeneous medium. One of these relations leads to the 'reflection-to-transmission' transform with applications in seismic imaging schemes that account for internal multiple reflections. The other relation leads to the 'transmission-to-reflection' transform with applications in acoustic daylight imaging.

References

Berkhout, A. J., 1982, Seismic migration. Imaging of acoustic energy by wave field extrapolation: Elsevier.

Claerbout, J. F., 1968, Synthesis of a layered medium from its acoustic transmission response: Geophysics, **33**, 264–269.

de Hoop, A. T., 1988, Time-domain reciprocity theorems for acoustic wave fields in fluids with relaxation: J. Acoust. Soc. Am., **84**, 1877–1882.

Fokkema, J. T., and van den Berg, P. M., 1993, Seismic applications of acoustic reciprocity: Elsevier, Amsterdam.

Herman, G. C., 1992, Estimation of the inverse acoustic transmission operator of a heterogeneous region directly from its reflection operator: Inverse Problems, **8**, 559–574.

Rickett, J., and Claerbout, J. F., 1999, Acoustic daylight imaging via spectral factorization: Helioseismology and reservoir monitoring: 69th Annual Internat. Mtg., Soc. Expl. Geophys., Expanded Abstracts, 1675–1678.

Verschuur, D. J., Berkhout, A. J., and Wapenaar, C. P. A., 1992, Adaptive surface-related multiple elimination: Geophysics, **57**, no. 9, 1166–1177.

Wapenaar, C. P. A., and Grimbergen, J. L. T., 1996, Reciprocity theorems for one-way wave fields: Geoph. J. Int., **127**, 169–177.

Wapenaar, C. P. A., and Herrmann, F. J., 1993, True amplitude migration taking fine-layering into account: 63rd Annual Internat. Mtg., Soc. Expl. Geophys., Expanded Abstracts, 653–656.

Weglein, A. B., Matson, K. H., Foster, D. J., Carvalho, P. M., Corrigan, D., and Shaw, S. A., 2000, Imaging and inversion at depth without a velocity model: theory, concepts and initial evaluation: 70th Annual Internat. Mtg., Soc. Expl. Geophys., Expanded Abstracts, 1016–1019.

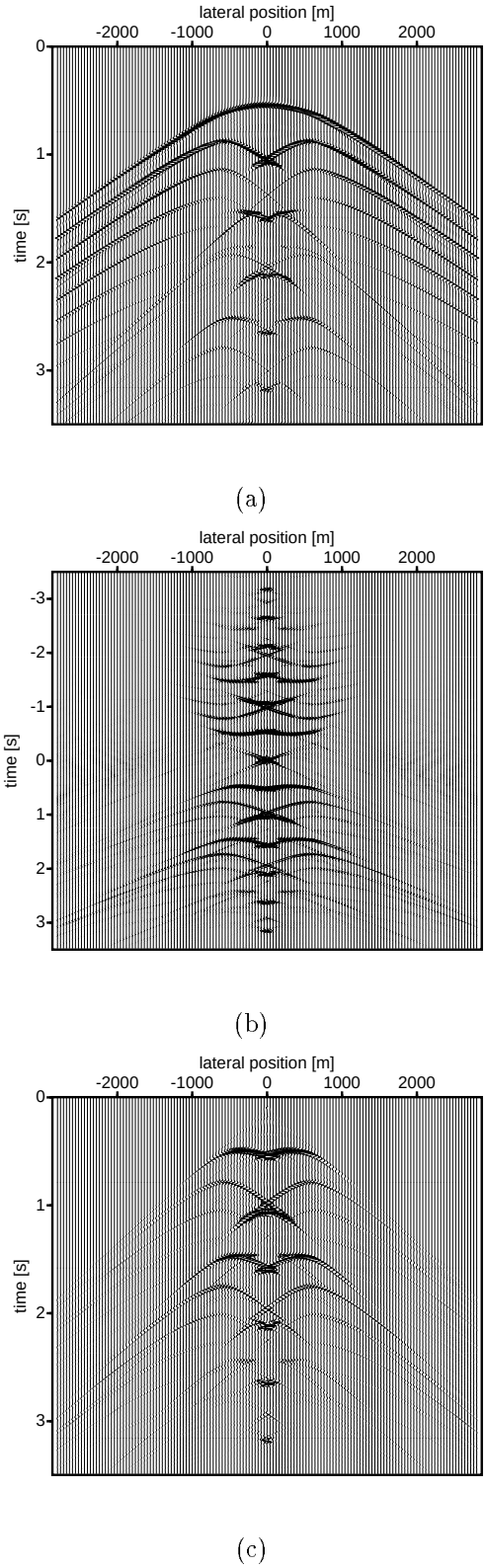

Fig. 19: Illustration of equation (41) for the 2-D medium in Figure 18. (a) Transmission response. (b) Result of the integral in the right-hand side of equation (41). (c) Causal part of the data in (b), after muting the bandlimited delta function. This is the reflection response $R^+(\mathbf{x}_A,\mathbf{x}_B,\omega)$.